Proceedings of the 37th Chinese Control Conference
July 25-27, 2018, Wuhan, China

Pipeline Scene Reconstruction Based on Image Mosaicing

Zishu Gao[1,2], En Li[1], Lei Yang[1,2], Zize Liang[1]

1. The State Key Laboratory of Management and Control for Complex Systems, Institute of Automation Chinese Academy of Sciences, Beijing 100190, China
E-mail: en.li@ia.ac.cn

2. The University of Chinese Academy of Sciences, Beijing 100049, China
E-mail: gaozishu2016@ia.ac.cn

Abstract:
Robots should be able to perceive the surroundings in the complicated and unknown environment before carrying out further navigation. Consequently, environmental reconstruction is the premise for the robot autonomous operations. In this paper, a pipeline scene reconstruction method based on image mosaicing is proposed for cylindrical pipeline environment. With a wide-angle camera, the image sequence of the pipeline environment is captured. In order to obtain intuitional environmental information around the pipeline, an unwrapped model is proposed to unfold the distorted raw image to corrected flat surface image. By utilizing ORB (Oriented FAST and Rotated BRIEF) and weighted smoothing blending algorithm, image mosaicing with sequence frames are performed to realize scene reconstruction. The experimental results demonstrate that the proposed algorithm can achieve seamless stitching of pipeline image, and the number of keypoints is prominently decreased in comparison to that of FAST operator, while the quality of keypoints is improved. Compared with the classical SIFT and SURF operator, the time-consuming of the algorithm is improved about 2.5 times, which is more suitable for real-time environmental reconstruction.

Key Words: scene reconstruction, image unwrapping, ORB, image mosaicing

1 Introduction

A variety of pipelines are the important way to achieve material transport in industry, these pipelines will lead to cracks perforation and scaling after a long period of use, so pipeline detection and maintenance is critical in order to guarantee long-term continuous use [1]. As the pipeline environment is narrow, complicated and dangerous, it is intensely difficult to carry out the manual inspection for the pipeline environment, and the robot is gradually becoming a kind of ideal pipeline inspection and maintenance equipment. In order to complete autonomous navigation for robots in pipeline environment, it is essential to reconstruct the pipeline. In particular, panoramic observation of pipeline environment will directly improve robot navigation control and operation quality.

In the pipeline reconstruction, the selection of sensors has a direct impact on the reconstruction effect.In the early work [2], pinhole camera is installed on the robot, and the image obtained can reflect the state of the pipeline. Nevertheless, due to the particularity of the pipeline structure, the image can merely get about 70° to 90° angle,which takes a lot of human resources to integrate these images into 360° panoramic images. The entire process is time-consuming and too complicated, affecting the operating efficiency. The development of fish-eye lens has become the technical support to cope with these issues.Fish-eye lens has very short focal length and viewing angle close to 180°. It has wide-angle characteristics, a picture can show the information on horizontal direction of 360°, so it has an evident advantage compared to ordinary cameras [3].

We install fish-eye lens on the robot, and continuously acquire video of the pipeline environment with the movement of the robot in the pipeline. Subsequently the system will get the video frame into images, finally we mosaic images and reconstruct pipeline. Image mosaicing is a key step in the process of environmental reconstruction, including spatial registration, plane projection and blending.

In recent years, image registration and image blending method are foundation of image mosaicing technology. Image registration establishes geometric relationship between a pair of images depicting the same scene. Image Blending is to eliminate image distortion and synthesize a seamless image of the overlapped image. At present, image registration methods are basically divided into area-based methods and feature-based methods [4],[5]. Area-based methods operate the gray information of the image directly, establish the similarity measure between the image to be registered and the reference image, find the transformation model parameters that make the similarity measure achieve the optimal value. Generally, area-based methods are grouped into normalized cross correlation-based method [6] and mutual information-based method [7]. The disadvantage of these methods is that if the image overlapped area is smaller, speed of registration will be very slow and the error is obvious, so it is limited for some applications. The feature-based algorithm has been studied by quite a few scholars. It depends on efficient image feature extraction, feature matching between images to calculate the geometric transform and complete the registration. Among the feature-based registration algorithms, Harris corner detector [8], FAST corner detector [9], SIFT feature detector [10], SURF feature detector [11] and ORB feature detector [12] are common. Harris operator is simple and accurate, but the choice of mask size requires sufficient prior knowledge. Once there are great rotation changes between the images, it will cause mosaicing to generate ghosting. FAST operator is precise and more efficient than Harris, however, the selection of threshold becomes the challenge and it is not robust against high intensity noise and increased image variability. SIFT operator has important properties including scale invariant, rotation invariant and affine invari-

This work is supported by National Natural Science Foundation (U1713224) and the National Key Research and Development Plan (2017YFD0701401).

Authorized licensed use limited to: INSTITUTE OF AUTOMATION CAS. Downloaded on September 23,2020 at 09:32:53 UTC from IEEE Xplore. Restrictions apply.

ant, especially with efficient and accurate detection effect for high resolution images. But its time consumption is extremely long, which is the important problem many scholars try to solve. SURF operator improves significantly over the above operators, and it's suitable for real-time splicing applications, although it is not ideal in the scene of more lighting changes and color changes. ORB operator is a combination of FAST corner detection and BRIEF descriptor. It has stable rotation invariance, low sensitivity to noise, fast calculation speed and is suitable for real-time detection, so it is suitable at present.

In this paper, according to the special environment of pipeline system, we use fish-eye lens to collect the images and expand them based on pipeline image unwrapped model. We use the ORB operator and weighted smoothing blending algorithm to realize image mosaicing, which has the characteristics of fewer keypoints and higher efficiency. The goal of this paper is to reconstruct pipeline environment automatically without any prior knowledge.

2 Scene reconstruction model

2.1 fish-eye lens imaging model

The Fish-eye lens imaging model is a linear camera model for projecting the surface of a space object onto the imaging plane. As shown in Figure 1, the linear Camera model contains an internal parameter matrix and an external parameter matrix, and the projection matrix of the camera is described as:

$$\lambda \begin{bmatrix} u \\ v \\ 1 \end{bmatrix} = \begin{bmatrix} f & 0 & u_0 & 0 \\ 0 & f & v_0 & 0 \\ 0 & 0 & 1 & 0 \end{bmatrix} \begin{bmatrix} R & T \\ 0 & 1 \end{bmatrix} \begin{bmatrix} X_w \\ Y_w \\ Z_w \\ 1 \end{bmatrix} \quad (1)$$

where f is the focal length, (u_0, v_0) is the intersection point of the optical axis center line and the imaging plane. R and T respectively represent rotation matrix and translation matrix of the coordinate transformation from the camera coordinate system to the world coordinate system, (X_w, Y_w, Z_w) is the coordinate of a point in the world coordinate system, (u, v) is the coordinate of imaging points in the imaging plane, λ is the scale factor.

2.2 equidistance projection model

Linear camera model is determined as:

$$r = f \tan\theta \quad (2)$$

Many people study fish-eye lens projection model[13], it is mainly composed of stereographic projection, equal Angle projection, orthogonal projection, equidistance projection [14]. The most commonly used is the equidistance projection model, and it is expression as below:

$$r = f\theta \quad (3)$$

The linear camera model and the equidistance projection model schematic diagram are shown in Fig. 1. θ is the angle between the incident beam and the main axis, r is the center of the image to the imaging point distance, f is the focal length. In the linear camera model, the light that is emitted by point M in the three-dimensional space does not have any deflection, and it continues to be projected onto the imaging plane, that is, point m' in the figure. However for fish-eye lens, the light emitted by point M will have a typical deviation, the distance from the image point of the fish-eye lens to the image center will be smaller than that of linear camera. Therefore, a larger radial distortion is introduced, shown in point m.

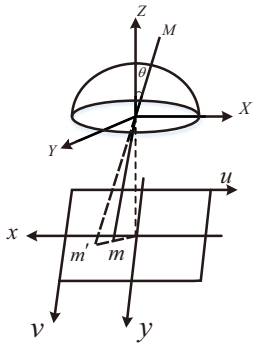

Fig. 1: equidistance projection model

In this paper, the fish-eye image needs to be expanded, and it will be corrected in accordance with the equidistance projection model.

2.3 pipeline image unwrapped model

The expansion process of pipeline images taken by the fisheye lens is dissimilar from that in the usual environment. In this paper, a new unwrapped model for pipeline structure is proposed, which can effectively improve the accuracy of pipeline expansion.

Taking the center of the circle as the center in the pipeline image, pixels of the circle corresponding to the different radii reflect the pixel distribution on the contour of the inner wall of the pipeline. Accordingly, the pipeline image expansion needs to map the image to the cylinder plane, subsequently the cylinder plane to the unwrapped image.

Pipeline image unwrapped model is shown in Fig. 2, point O is the fish-eye lens, the focal length of the fish-eye lens is f, the height of pipeline wall is H, the radius is R, point P is on the pipeline image, P is mapped to point P' on the wall of the pipeline, and the Angle between P' and the inner wall of the pipeline O_1A_1 is φ. d_x, d_y is the physical size of the horizontal and vertical coordinates in the imaging coordinate system, d_u, d_v are the pixel distortion of the horizontal and vertical coordinates, caused by the fish-eye lens. The corresponding point of point P' in pipeline expansion figure is P''.

$$\begin{cases} x = (u - u_0 - d_u)d_x \\ y = (v - v_0 - d_v)d_y \\ r = \sqrt{x^2+y^2} \end{cases} \quad (4)$$

According to the fish-eye lens equidistance projection model:

$$\begin{cases} \theta_1 = \frac{r_1}{f} = \frac{\sqrt{((u_1-u_0-d_u)d_x)^2+((v_1-v_0-d_v)d_y)^2}}{f} \\ \theta_2 = \frac{r}{f} = \frac{\sqrt{((u-u_0-d_u)d_x)^2+((v-v_0-d_v)d_y)^2}}{f} \\ L = \frac{R}{\tan\theta_1} \\ H_1 + L = \frac{R}{\tan\theta_2} \end{cases} \quad (5)$$

Authorized licensed use limited to: INSTITUTE OF AUTOMATION CAS. Downloaded on September 23,2020 at 09:32:53 UTC from IEEE Xplore. Restrictions apply.

Obtained by the above formula:

$$P_y'' = H_1 = \frac{R}{\tan\theta_2} - \frac{R}{\tan\theta_1} \tag{6}$$

The angle of P' and the pipeline wall O_1A_1 is φ,thus,

$$P''_x = \frac{360^\circ - \varphi}{360^\circ} * 2\pi R \tag{7}$$

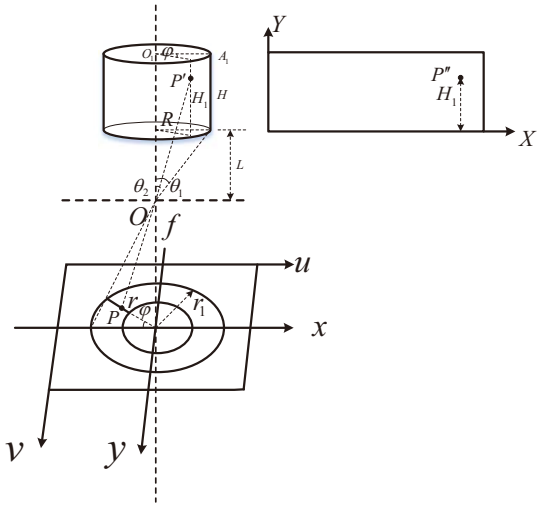

Fig. 2: pipeline image unwrapped model

3 Scene reconstruction based on image mosaic

To reconstruct the pipeline based on image stitching, we present some steps. Firstly image preprocessing also called random noise removal, which ensures that image has the calibration accuracy of pixel level. The next step is image unwrapping with image correction. Image registration and image blending are the core and focus of this process. Image registration [16] requires finding transformation relation of the two images, and makes the overlapping parts of the two images blending perfectly. Image fusion [17] is to improve the image seams due to differences in intensity scale, by removing unnecessary information to make stitching boundary traces smooth, and without losing important information of the original image.

3.1 image preprocessing

Image preprocessing mainly achieves image denoising, and we perform median filtering on images. Median filter is a nonlinear smoothing filter, which can overcome the fuzzy problem of image details brought by linear filter under certain conditions and enhance the image. The algorithm uses a sliding window with nine points to sort the intensity values in this window, and then assign the values to the center point.It is defined as:

$$\begin{aligned} f'(x,y) = median\{&f(x-1,y-1), f(x,y-1),\\ &f(x+1,y-1), f(x-1,y), f(x+1,y), f(x-1,y+1),\\ &f(x,y+1), f(x+1,y+1)\} \end{aligned} \tag{8}$$

Median filter can quickly filter each frame of image to reduce the interference of noise on the image, and it can save most of the important details of the image, making image registration achieve better results.

3.2 image unwrapped

Image unwrapped is the basis of image mosaicing, we obtain horizontal and vertical coordinates of the expanded picture using above pipeline image unwrapped deduction. Since pipeline image creates non-linear compression in the lateral field of view, dense distribution of pixels after the unfolding image is different, additionally, the image pixels outside the pipeline should also be considered, so we use bilinear interpolation to solve these problems. Interpolation function f satisfies quadratic function, assuming that a point p, according to its four adjacent integer pixels' gray value $P_{11}(x_1,y_1), P_{12}(x_1,y_2), P_{21}(x_2,y_1), P_{22}(x_2,y_2)$, we interpolate in the x and y directions respectively,first in x direction,

$$\begin{cases} f(Q_1) = \frac{x_2-x}{x_2-x_1} f(P_{11}) + \frac{x-x_1}{x_2-x_1} f(P_{21}) \\ f(Q_2) = \frac{x_2-x}{x_2-x_1} f(P_{12}) + \frac{x-x_1}{x_2-x_1} f(P_{22}) \end{cases} \tag{9}$$

where $Q_1 = (x,y_1), Q_2 = (x,y_2)$. Then in y direction,

$$P(x,y) = \frac{y_2-y}{y_2-y_1} f(Q_1) + \frac{y-y_1}{y_2-y_1} f(Q_2) \tag{10}$$

The basis of unwrapping process is to find the center of the pipeline image, we utilize the Hough transform to detect the center of the circle [17],[18]. Hough transform uses the global features of image to connect edge pixels to form the region closed boundary, it converts the circle on the X-Y plane to the a-b-r parameter space, describes the point in the parameter space, and achieves the goal of detecting the edge of the image.The method calculates all points that may fall on the edge of the statistics, according to the statistical results of the data to determine the degree of belonging to the edge.

We adopt Hough gradient algorithm for detection, the algorithm is listed in Algorithm 1.

There are some disturbances and uncertainties in the use of single picture to obtain the center coordinates. We rotate the fish-eye lens at the pipe mouth at a fixed angle, and write down a numerical value for the center each time. Rotate n times and ask for their arithmetic mean as the final center coordinates.

According to this principle, we detect the circle in the pipeline image, radius of the cylinder is R, the distance from the fish-eye lens to the starting point of calculation in the three-dimension space is L, the focal length of fish-eye lens is f. We scan the pixels along the azimuth and radius in the image coordinate, and accomplish the unwrapping. The results are as shown in Fig. 3.

3.3 image registration

The key step of image registration is to calculate the feature points of the image, and detection speed of feature points is closely related to the time cost of registration. At present, commonly used feature extraction operators include SIFT, SURF, FAST, ORB and so on. ORB operator is an image local feature descriptor which is invariant to rotation. It is called SIFT and SURF effective substitute, because it is computationally efficient and insensitive to noise. In this paper, ORB operator is used to extract the features of unwrapped images.

Authorized licensed use limited to: INSTITUTE OF AUTOMATION CAS. Downloaded on September 23,2020 at 09:32:53 UTC from IEEE Xplore. Restrictions apply.

Algorithm 1 Framework of Hough gradient algorithm for detection.

Input: grayscale image; cenThreshold; minRadius; maxRadius;
Output: vector of found circles;

```
Build a binary image utilizing Canny algorithm;
Build a 2 dimensional accumulator;
for each pixel do
    Calculate the neighborhood gradient using Sobel operator;
end for
for all non-zero points in the binary image do
    Draw lines along gradient direction;
    Count the points passed through the line;
    Calculate the distance from all non-zero points to the center and sort them;
end for
for radius(i) = minRadiustomaxRadius do
    for radius(j) = minRadiustomaxRadius do
        if |radius(i) − radius(j)| ≤ cenThreshold then
            radius(i) = radius(j).
        end if
    end for
end for
for radius(i) = minRadiustomaxRadius do
    lineDensity(k) = points/radius(i).
end for
radius = max_radius lineDensity.
```

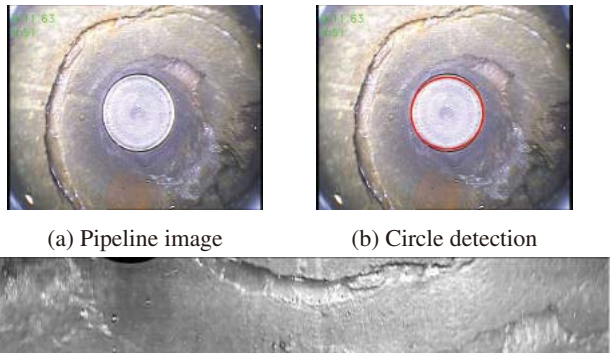

(a) Pipeline image (b) Circle detection

(c) Unwrapped image

Fig. 3: Image unwrapped process

ORB operator combines FAST corner detector with BRIEF feature descriptor [19], and makes improvements on the original basis. Firstly, the keypoints are detected by FAST operator, since the FAST operator does not propose the method of measuring the corner points, Harris corner metric method is adopted. The response function of the Harris corner point is defined as:

$$R = \det M - \alpha(traceM)^2 \tag{11}$$

Select N feature points with the maximum response value of Harris. ORB operator obtains the direction of the keypoints by Intensity centroid method. For a feature point P, we define the moments of a patch as:

$$m_{pq} = \sum_{x,y} x^p y^q I(x,y) \tag{12}$$

where $I(x,y)$ is intensity value in (x,y), we can calculate the centroid:

$$C = (\frac{m_{10}}{m_{00}}, \frac{m_{01}}{m_{00}}) \tag{13}$$

The angle between the keypoint and the centroid is defined as the direction of FAST keypoint:

$$\theta = \arctan(m_{01}, m_{10}) \tag{14}$$

In order to improve the rotation invariance of the method, we need to ensure that x and y are in the circular region with radius r. In addition, ORB operator refers to BRIEF descriptor and develops into Steered BRIEF with rotation invariance. It selects n pairs of points in the neighborhood range of the keypoint, and calculates the binary intensity value of n pairs of points, a binary intensity value is defined by:

$$\tau(p;x,y) = \begin{cases} 1 & p(x) < p(y) \\ 0 & p(x) \geq p(y) \end{cases} \tag{15}$$

where $p(x)$ is the intensity of p at a point x, the binary intensity value of length n is defined as:

$$f_n(p) := \sum_{1 \leq i \leq n} 2^{i-1} \tau(p;x,y) \tag{16}$$

Next, add a rotation invariance to the BRIEF, and a binary intensity value of length n is generated by n pairs of points around the feature points. Now these 2n points are formed into a matrix S, which is defined as:

$$S = \begin{pmatrix} x_1 & x_2 & \dots & x_{2n} \\ y_1 & y_2 & \dots & y_{2n} \end{pmatrix} \tag{17}$$

we construct a steered version S_θ of S using the orientation θ and the corresponding rotation matrix R_θ, it is defined by:

$$S_\theta = R_\theta S \tag{18}$$

where $R_\theta = \begin{bmatrix} \cos\theta & \sin\theta \\ -\sin\theta & \cos\theta \end{bmatrix}$

So the improved BRIEF descriptor is:

$$g_n(p,\theta) := f_n(p) \,|(x_i.y_i) \in S_\theta \tag{19}$$

We adopt the Brute-force matcher algorithm to match the keypoints, and find out the two most similar features in the two images and connect them. In order to make the matching more efficient, we need to further select the matching points. In this paper, Lowe's algorithm in SIFT article [10] is utilized to exclude the keypoints of mismatch, making the matching more stable. This method proposes the Euclidean distance of the keypoint eigenvector as the similarity measure in the two images, and is defined as:

$$\frac{d_{i0}}{d_{i1}} < \lambda \tag{20}$$

Take one keypoint i in the first image and find the first two keypoints closest to the European distance in the second image, in both of these keypoints, the match is accepted if the nearest distance is divided by less than a certain threshold.

The results of feature detection and matching based on ORB operator are shown in Fig. 4, from 4(a), 4(b), we

Authorized licensed use limited to: INSTITUTE OF AUTOMATION CAS. Downloaded on September 23,2020 at 09:32:53 UTC from IEEE Xplore. Restrictions apply.

can see that ORB operator detect enough feature points in pipeline image. The initial matching is shown in 4(c), there are a large number of matching pairs, including some error. We use the Lowe's algorithm and set λ to 0.55. The improved matching is shown in figure 4(d).

(a) Keypoints detection1

(b) Keypoints detection2

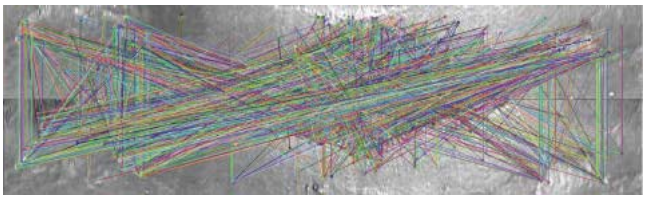

(c) Initial matching

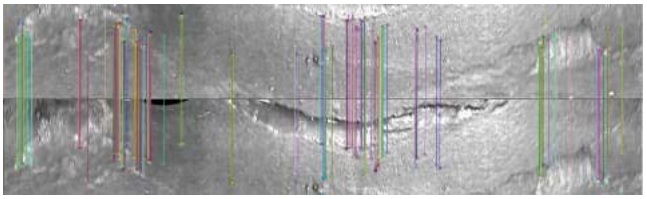

(d) final matching

Fig. 4: Image matching process

3.4 image blending

Due to the illumination, the difference of the intensity and the degree of deformation occur in the overlapping part. The goal of image blending is to eliminate the discontinuity of the light intensity in the overlapping area and realize the smooth transition[17]. We adopt the weighted smoothing algorithm, which uses the gradient method to fuse the transition region, so that the blended image has visual consistency. Assuming that we blend N images,then,

$$P = \frac{\sum_{i=1}^{N} P_i w_i}{\sum_{i=1}^{N} w_i} \tag{21}$$

Where P_i denotes the pixels of the ith image in the area on both sides of the seam line, w_i is the weight value of P_i, which indicates the distance from the current pixel to the nearest boundary of the nth expanded image. This method is simple and requires short time to meet the computational efficiency requirements.

4 experiments and discussions

Pipeline reconstruction system needs image acquisition, image preprocessing, image mosaic, image preservation, and we finally get a seamless image. The flow chart of pipeline reconstruction is shown in Fig. 5.

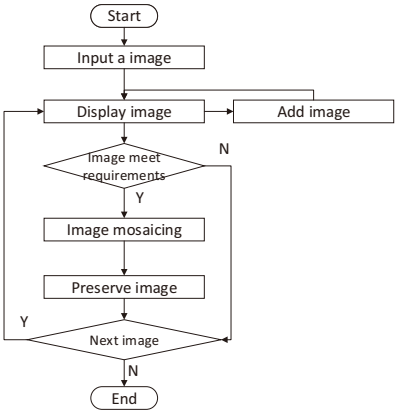

Fig. 5: Flow chart of pipeline reconstruction

In order to verify the detection, mosaicing effect and computational efficiency of ORB operators, we select two pictures to do stitching experiment, and stitching results are shown in Fig. 6.

(a) Pipeline image1

(b) Pipeline image2

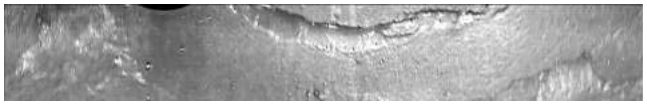

(c) Unwrapped image1

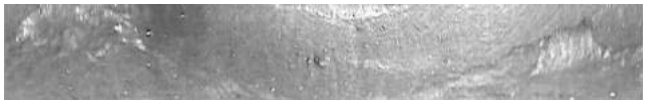

(d) Unwrapped image2

(e) Image mosaicing

Fig. 6: ORB operator image mosaicing

At the same time, we use SIFT operator, SURF operator, FAST operator to do the same stitching experiments, the results are shown in Fig. 7.

It can be seen that all the four operators have satisfied results, there is almost no apparent trace after eliminating the overlapping part of the boundary, which is convenient for the robot to detect.

These experiment compare and analyze the efficiency of four operators. Table 1 shows detection result and processing time. In terms of the number of keypoints detected, FAST detected the most number, SIFT and SURF detection number was similar, and the number of keypoints detected by ORB was the least. From the view of test effect, the quality of the keypoints detected by ORB operator is very high,

Authorized licensed use limited to: INSTITUTE OF AUTOMATION CAS. Downloaded on September 23,2020 at 09:32:53 UTC from IEEE Xplore. Restrictions apply.

(a) SIFT operator

(b) SURF operator

(c) FAST operator

Fig. 7: SIFT, SURF, FAST operator image mosaicing

which satisfies the need of keypoints matching. In addition, FAST has a great improvement in computational efficiency compared to SIFT, SUFT. As a FAST improvement, ORB consumes very little time and has the highest quality at the same time. It lays a foundation for keypoints matching and image mosaicing.

Table 1: Feature points number and processing time

Operator	Feature points number	Processing time[ms]
SIFT	1922-2371	1152.84
SURF	1514-1868	152.67
FAST	2175-3610	13.01
ORB	1355-1498	36.46

The quality of matching points is more important for image mosaicing. In the precondition of satisfying the experimental requirements, appropriate quantity and high quality matching pairs can reduce the time cost in the later processing. Table 2 compares the initial matching pairs and final matching pairs after removing mismatches. It can be seen that ORB operator has the least improved matching points, and the high-quality matching makes the registration very satisfactory.

Table 2: Initial and final matching pairs

Operator	Initial matching pairs	Final matching pairs
SIFT	1922	297
SURF	1514	289
FAST	2175	335
ORB	1355	191

From the above experiments, we can see that all the four operators have satisfying mosaicing results, Meanwhile, ORB operator has the highest computational efficiency, and it is insensitive to noise, so ORB operator becomes the most approving method.

5 Conclusion

This paper designs a reconstruction algorithm based on image mosaicing in order to meet the demand of robot autonomous navigation in pipeline environment. We propose a unique image expansion model, and combine ORB feature detector and weighted smoothing blending algorithm for image mosaicing. The system with fish-eye lens data acquisition platform can accomplish the reconstruction of pipeline automatically without any prior knowledge.

References

[1] S. Jerban, MM. Moghaddam, On The In-pipe Inspection Robots Traversing Through Elbows, *International Journal of Robotics, Theory and Applications*, 4(2): 19–27,2015.

[2] T. Takano, S. Ono, Y. Matsushita ,et al, Super resolution of fisheye images captured by on-vehicle camera for visibility support, *Vehicular Electronics and Safety , 2015 IEEE International Conference on*, 2015: 120–125.

[3] W. Feng, B. Zhang, Z. Cao, Omni-Directional Vision Parameter Calibration and Rectification Based on Fish-Eye Lens, *Journal of Tianjin University*, 5: 007,2011.

[4] D. Ghosh, N. Kaabouch, A survey on image mosaicing techniques,*Journal of Visual Communication and Image Representation*, 34: 1-11,2016.

[5] TE. Tseng, AS. Liu, PH. Hsiao, Real-time people detection and tracking for indoor surveillance using multiple top-view depth cameras,*Intelligent Robots and Systems*, 2014: 4077–4082.

[6] JP. Lewis, Fast normalized cross-correlation,*Vision interface*,10(1): 120-123,1995.

[7] P. Viola, WM. Wells, Alignment by maximization of mutual information,*International journal of computer vision*, 24(2): 137-154,1997.

[8] C. Harris, W. Stephens, A combined corner and edge detector,*Alvey vision conference*,15(50): 10.5244,1998.

[9] E. Rosten, T. Drummond, Machine learning for high-speed corner detection,*Computer VisionCECCV 2006*,2006: 430-443.

[10] DG. Lowe, Distinctive image features from scale-invariant keypoints,*International journal of computer vision*,60(2): 91-110,2004.

[11] H. Bay, T. Tuytelaars, L. Van Gool, Surf: Speeded up robust features,*Computer visionCECCV 2006*,2006: 404-417.

[12] E. Rublee, V. Rabaud, K. Konolige et al,ORB: An efficient alternative to SIFT or SURF,*Computer Vision (ICCV), 2011 IEEE international conference on*,2011: 2564-2571.

[13] J. Kannala, S. Brandt, A generic camera model and calibration method for conventional, wide-angle, and fish-eye lenses,*IEEE Transactions on Pattern Analysis and Machine Intelligence*,28(8): 1335-1340,2006.

[14] C. Hughes, P. Denny, M. Glavin et al,Equidistant fish-eye calibration and rectification by vanishing point extraction,*IEEE Transactions on Pattern Analysis and Machine Intelligence*,32(12): 2289-2296,2010.

[15] Q. Liao, Research on panoramic ring lens imaging expansion algorithm,*Science and Technology Information*,(10):134-135,2012

[16] KSV. Prathap, SAK. Jilani, PR. Reddy, A critical review on Image Mosaicing,*Computer Communication and Informatics (ICCCI), 2016 International Conference on*,2016: 1-8.

[17] N. Gracias, M. Jilani, S. Reddy et al ,Fast image blending using watersheds and graph cuts,*Image and Vision Computing*,27(5): 597-607,2009.

[18] DH. Ballard, Generalizing the Hough transform to detect arbitrary shapes,*Pattern recognition*,13(2): 111-122,1981.

[19] M. Calonder, V. Lepetit, C. Strecha et al ,Brief: Binary robust independent elementary features,*Computer VisionCECCV 2010*,2010: 778-792.

Authorized licensed use limited to: INSTITUTE OF AUTOMATION CAS. Downloaded on September 23,2020 at 09:32:53 UTC from IEEE Xplore. Restrictions apply.